Subwavelength optical dipole trap for neutral atoms using a microcapillary tube tip

2017 J. Phys. B: At. Mol. Opt. Phys. 50 045005

(http://iopscience.iop.org/0953-4075/50/4/045005)

IOP Publishing Journal of Physics B: Atomic, Molecular and Optical Physics
J. Phys. B: At. Mol. Opt. Phys. **50** (2017) 045005 (8pp) https://doi.org/10.1088/1361-6455/aa5518

Subwavelength optical dipole trap for neutral atoms using a microcapillary tube tip

Pengfei Zhang[1,2], **Gang Li**[1,2] **and Tiancai Zhang**[1,2]

[1] State Key Laboratory of Quantum Optics and Quantum Optics Devices, Institute of Opto-Electronics, Shanxi University, Taiyuan 030006, People's Republic of China
[2] Collaborative Innovation Center of Extreme Optics, Shanxi University, Taiyuan, Shanxi 030006, People's Republic of China

E-mail: zhangpengfei@sxu.edu.cn

Received 12 August 2016, revised 11 December 2016
Accepted for publication 21 December 2016
Published 31 January 2017

Abstract

We propose a scheme for a state-insensitive optical dipole trap for single cesium atoms using a silica microcapillary tube tip. The end of microcapillary tube tip is flat. Simulations show that the trapping light beam output from microcapillary tube tip interferes and can form a subwavelength-trap with a full width at half-maximum of 0.67 μm. The trap is small enough to trap single atoms. The trap depth is more than 1 mK when the optical power of the trapping light guided by the microcapillary tube tip is only a few milliwatts. The effects of two imperfections, roughness of end surface and cutting angle, are estimated. The trapping depth for single atom trapping can be more than 1 mK when the average rms amplitude and average correlation length of tip surface roughness is smaller than 0.15 μm and the cutting angle is smaller than 16 degrees. Tip sizes on the order of microns are small enough to be combined within micro/nano structures for hybrid systems.

Keywords: optical dipole trap, single atoms, microcapillary tube tip

(Some figures may appear in colour only in the online journal)

In the last 20 years, single emitters have been a topic of great interest not only for fundamental physics but also for single photon sources [1], quantum entanglement [2] and quantum state manipulations [3], which are the key elements for quantum communication and quantum information applications [4]. Trapped single neutral atoms are ideal candidates, as their interactions with the environment are weak. Recently, cold neutral atoms or single atoms trapped in hybrid quantum systems [5–7] have attracted considerable attention. Strong interactions between atoms and nanostructure fields can be achieved when cold neutral atoms are trapped in the near field of a nanostructure [8–10].

However, it is still challenging to trap atoms close to the surface of nanostructures because of van der Waals forces, attractive atom-surface forces. Trapping and manipulating single neutral atoms can be achieved by a microscopic far-off-resonance optical dipole trap (FORT) [11]. A conventional method employs high numerical-aperture objectives with spherical or aspherical lenses are used to get micrometer-scale FORTs [12–14]. Single atoms trapped in FORTs can be controlled with high accuracy and high numerical-aperture objectives can collect photons from single atoms efficiently. However, higher numerical apertures cause shorter working distances, which usually causes the problem of accessibility for trapping single atoms close to a hybrid system because of the huge lens body. Some new methods based on evanescent fields have been proposed and demonstrated experimentally. In 1991, atomic traps based on evanescent light were proposed [15] and demonstrated experimentally [16]. In 2004, Kien *et al* proposed a method for trapping atoms using the evanescent field of a nanofiber carrying a red-detuned laser beam and a blue-detuned laser beam, called two-color traps [17]. Two-color traps based on nanofibers were demonstrated by the Rauschenbeutel [18] and Kimble [19] groups experimentally in 2010 and 2011. Recently, Daly *et al* proposed an optical dipole trap inside a nanofiber based on a hollow, rectangular slot cut through an optical nanofiber [20]. Instead of utilizing the trapping lasers propagating in the nanofibers, a single atom trap using an incident laser beam perpendicular to the fiber axis was also studied which showed that the

nanofiber could focus the incident light and form a dipole trap [21].

An increasing number of proposals and methods based on micro/nano structures are used for atom manipulation. Micro/nano structures have played an important role in optical dipole traps, especially in hybrid systems [22]. In 2013, Thompson *et al* demonstrated that a single atom could be trapped using a tightly focused optical beam that is retro-reflected from a nanoscale object [8]. Garcia *et al* demonstrated a fiber-coupled optical tweezer to trap a single atom [23]. Conventional aspherical lenses were used in those experiments. Since the first demonstration of optical trapping for particles by Ashkin in 1970 [24], many types of fiber tip have been fabricated and used for trapping particles [25–33]. These methods are naturally considered to be useful to trap single neutral atoms. In 2009, Chang *et al* proposed a method for trapping and manipulation of individual atoms using a metallic nanotip similar to optical fiber tips [34]. In 2010, J Fu *et al* experimentally demonstrated subwavelength focusing using a tapered microtube [35]. In 2014, Kato *et al* experimentally demonstrated that a hemispherically shaped fiber tip can be fabricated by annealing a fiber taper and can collect photons from an emitter placed near the beam waist into the fundamental guided mode efficiently [36]. This technique may be used to trap single atoms [36]. However, sufficient distance is needed between the traps and the tip surfaces to avoid the effects of van der Waals forces for single atom trapping. In addition, the fabrication of hemispherical microfiber tips is not easy.

In this paper, we propose and demonstrate a state-insensitive dipole trap for single cesium atoms using a silica microcapillary tube tip. It is shown that the guided trapping light beam output from a silica microcapillary tube tip can interfere and a trap with minimum potential is formed that is far enough away from the end surface of microcapillary tube tip. In addition, the hollow structure of microcapillary tube tips can reduce the effects of van der Waals forces. The size of the trapping well is smaller than the sizes of focused spots by using already-reported high numerical aperture optics. At this size regime, it can be used to trap single atoms with strong confinement. The microcapillary tube tip with the size of a few micrometers is so small that it can be integrated into a hybrid system. Microcapillary tube tips with flat end surfaces are easy to fabricate. In this paper, the wavelength of the trapping light we use is the 'magic wavelength'. The trapping light with magic wavelength causes the same AC-stark shift to the ground state $6S_{1/2}$ and the excited state $6P_{2/3}$ of the cesium atom, which means that the relevant atomic properties remain immune to strong perturbations by optical trapping fields when the atoms are trapped by magic wavelength light [37]. The trapping light is red-detuned for the D2 transition line of cesium atoms. We optimize the parameters and choose suitable inner/outer diameters of microcapillary tube tips to yield sufficient trap depth using a low optical power trapping light guided by the microcapillary. In contrast to conventional tools, our proposal provides a method for micro/nano structure-based laser trapping of cold atoms with more confinement. Hybrid systems combining single atom trapping and micro/nano structures are one of the difficulties in implementing the protocols of quantum information processing in experiments based on micro/nano structures. This method can be used not only in single emitter trappings for integrated quantum information processing, but also for optical tweezers in biology or chemistry control and sensing.

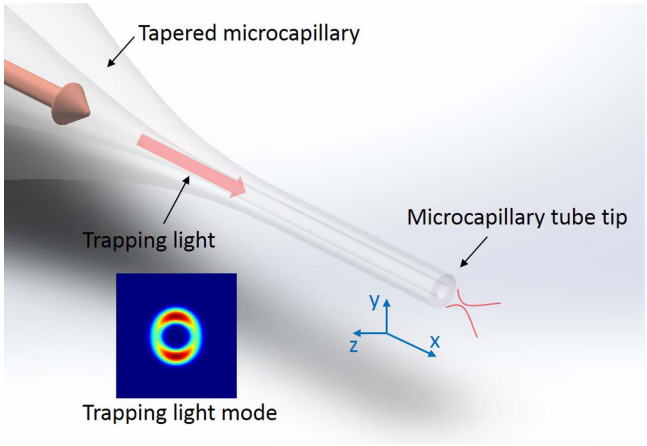

Figure 1. Schematic diagram of a microcapillary tube tip.

Figure 1 shows the diagram of a microcapillary tube tip schematically. A microcapillary tube tip is connected with a tapered capillary tube; a guided light propagates from the tapered capillary tube to the microcapillary tube tip as a trapping light. The end of the microcapillary tube tip is circular and flat. We consider that the refractive index in the silica capillary tube is 1.45 for the magic wavelength of cesium atoms of 935 nm. The guided modes of trapping light we use are fundamental TE mode, as shown in the inset of figure 1. We use the finite difference time domain (FDTD) method for numerical simulations to obtain electric field intensity distributions.

In figure 2, we present a typical electric field intensity distribution output from the microcapillary tube tip. Electric field intensities are normalized to the maximum intensity in the microcapillary tube. Figures 2(a) and (b) show the distributions in the *xy* and *xz* planes, respectively. The outer and inner diameters of the microcapillary tube tip are 4.0 μm and 1.5 μm, respectively. The size is comparable to the nanofiber structures we use in the next experiments. The trapping light wavelength is 935 nm. For the fundamental TE mode shown in the inset of figure 1, there are two patterns guided in the microtube body. The point with the maximum intensity output from the tip is generated by the interference of the two patterns output from the microtube body. The light spot with a maximum intensity is 3.2 μm away from the end surface of the tip. This light can form a trapping well and be used to trap cold atoms. The end surface of the tip is defined as zero of the *x*-axis. The vertical distance between the maximum intensity point and the end surface of the microcapillary tube tip is defined as the working distance. Figures 2(c) and (d) show the electric field intensity distributions along *y*- and *z*-axes, respectively, when x is 3.2 μm. Figure 2(e) shows the intensity distribution along the *x*-axis when y is 0 μm.

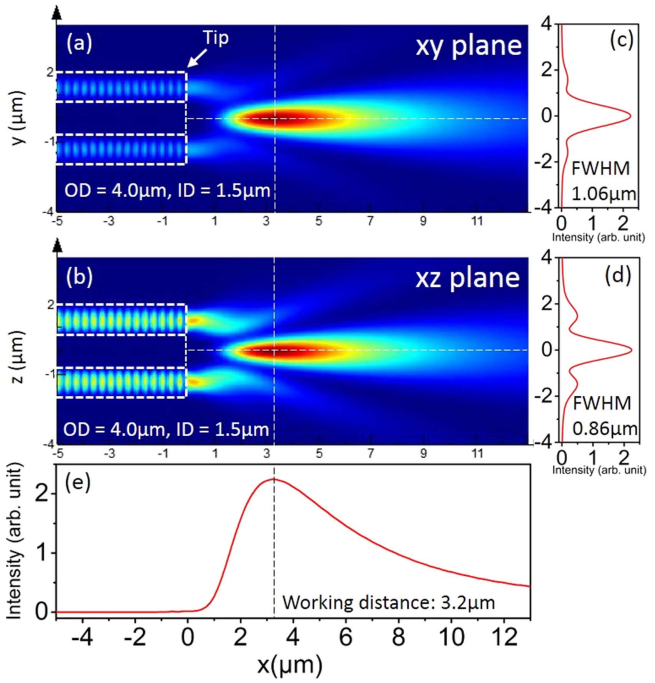

Figure 2. Typical electric field intensity distributions output from the microcapillary tube tip in the (a) *xy* and (b) *xz* planes. The outer diameter (OD) of the tip is 4.0 μm, while the inner diameter (ID) is 1.5 μm. The end surface of tip is at the zero of the *x*-axis. Electric field intensity distribution along the (c) *y*- and (d) *z*-axes when x is 3.2 μm (vertical white dash line shown in panel (a) and (b)). (e) Electric field intensity distribution along the *x*-axis when *y* is 0 μm (horizontal white dashed line shown in panels (a) and (b)).

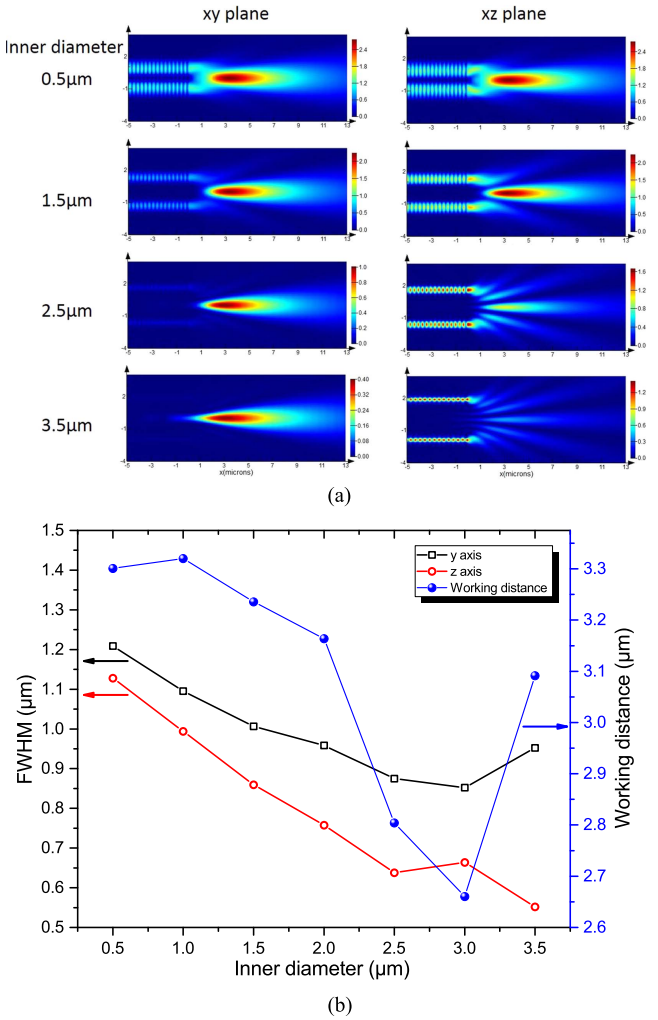

Figure 3. (a) Field intensity output from the microcapillary tube tip with various microcapillary tube tip inner diameters of 0.5, 1.5, 2.5, and 3.5 μm. (b) FWHMs of the trapping well along the *y*-axis (black open squares) and *z*-axis (red open circles) as a function of inner diameter. Blue solid circles are working distance versus the inner diameter. The outer diameter is 4.0 μm for all conditions. The wavelength of trapping light is 935 nm with fundamental TE mode guided by the microcapillary tube.

We analyzed the electric field intensity distributions with different inner diameters ranging from 0.5 μm to 3.5 μm, while maintaining the outer diameter at a constant 4.0 μm. The intensity distributions with diameters of 0.5, 1.5, 2.5, and 3.5 μm, are shown in figure 3(a). We can see that the microcapillary tube tip can form only one interference spot with a maximum intensity in the *xy* plane. However, more light spots are generated in the *xz* plane. The reason is that the distance between the two patterns of fundamental TE mode increases when the inner diameter of microtube increases from 0.5 μm to 3.5 μm with outer diameter 4.0 μm. In this case, the number of interference spots increases and the peak intensities decrease with increasing inner diameter. Only one interference spot is generated when the inner diameter is smaller than 2.5 μm in the *xz* plane. We examine the working distance and the full width at half maximum (FWHM) versus the inner diameter, as shown in figure 3(b), where black open squares and red open circles are the FWHMs along *y*- and z-axes, respectively. Larger inner diameters correspond to a smaller FWHM values. The inner diameter can be smaller than 1 μm, which can be used to confine and trap single atoms. The working distance decreases with increasing inner diameter (blue solid circles). However, when the inner diameter is 3.5 μm the working distance is abnormal because the thickness of tube corresponds to half of the trapping light wavelength. The working distance is far enough to avoid the effects of van der Waals interactions. We have calculated the optical dipole potentials to optimize the microcapillary tube tip design for cold atoms trapping according to the electric field intensity distributions as shown above.

The simulations above indicate that the output of microcapillary tube tip can form a point with very strong confinement of the light field, which implies the far-off-resonance optical trap for single neutral atom manipulation. High potential of the trap can be reached with a low input optical power of only a few milliwatts. When a cesium atom is placed into the output light from the tip, the dipole potential of an atomic state i with Zeema level m_i can be described by $U_i(\omega, p, m_i) = -\frac{1}{4}\alpha_i(\omega, p, m_i)|E|^2$ [11, 38]. The frequency of the trapping light is $\omega/2\pi$. p is 0 (the polarization of trapping light is approximate to linear polarization along the *y* axis because the *y*-component is much bigger than the other two components, *x* and *z*-components, two orders of magnitude). E is electric field and α_i is the reduced polarizability

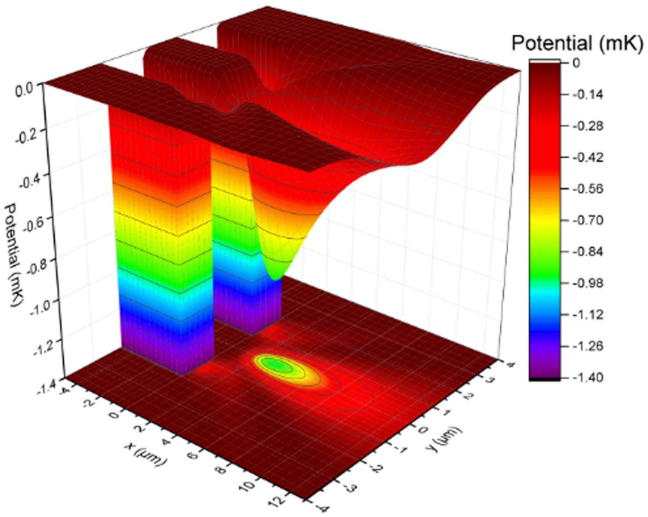

Figure 4. Three-dimensional color-map surface plot of the total potential in the *xy* plane with outer and inner microcapillary tube tip diameters of 4.0 μm and 1.5 μm, respectively. The wavelength of the trapping light is 935 nm. The effective dipole trap depth is 0.82 mK with a trapping light power of 6 mW.

which can be described by

$$\alpha_i(\omega, p, m_i) = 6\pi\varepsilon_0 c^3 \sum_{k,m_i} \frac{A_{ki}(2J_k+1)}{\omega_{ik}^2(\omega_{ik}^2-\omega^2)} \times \begin{pmatrix} J_i & 1 & J_k \\ m_i & p & -m \end{pmatrix}^2. \quad (1)$$

Here ε_0 is the permeability of vacuum and c is the speed of light. The expression within the large parentheses denotes a Wigner 3-j symbol. A_{ki} are the Einstein coefficients, $\omega_{ik}/2\pi$ is the transition frequencies and J is the involved angular momenta. In our simulations, eight transition lines are considered and all the parameter values can be taken from cesium atomic line data [39]. Dipole potentials can be obtained according to the electric field intensity distributions in the previous section.

Van der Waals potentials have an effect on effect on atoms when they are near the flat surface of the microcapillary tube tip. The van der Waals potential is given by $V_{\mathrm{VDW}} = -C_3/D^3$ approximately, where D is the distance from the tip surface to the atom. The value of the coefficient C_3 is 4.1 $\times$ 10^{-5} mK μm^3 [16, 40] for silica material.

The total potential can be given by combining the optical dipole potential and the van der Waals potential, described by $U_{\mathrm{total}} = U + V_{\mathrm{VDW}}$. Figure 4 shows a typical three-dimensional color-map surface plot of the total potential in *xy* plane with outer and inner microcapillary tube tip diameters of 4.0 μm and 1.5 μm, respectively. The power of trapping light guided by the microcapillary tube is 6 mW. 6 mW can generate 1 mK trap depth which is commonly used in single atom trapping experiments [11]. All the parameters are the same as in figure 2. The trapping well can be seen in figure 4. The microcapillary tube tip contributes a negative infinite potential. The minimum potential of the trapping well outside the tip is -0.96 mK, which can contribute the maximum depth of the dipole trap 0.96 mK. However, owing to the effects of the tip body end, there is a point with a potential of -0.14 mK between the trap center and the microcapillary tube tip body. We define the effective trap depth of the dipole trap is the potential difference between this point and the minimum potential of the trapping well. The effect of the tip body end reduces the trap depth. Therefore, the effective dipole trap depth is 0.82 mK which is smaller than the maximum depth of 0.96 mK.

Microcapillary tube tips have two important parameters. One is the ratio between the inner diameter and the outer diameter, while another is the value of the outer diameter. We sweep the two parameters to find the maximum effective dipole trap depth to optimize the traps. We study the total potentials by varying the inner diameter from 0.5 μm to 3.5 μm with the outer diameter a constant 4.0 μm. The results are shown in figure 5. Figures 5(a) and (b) show the trapping well potentials versus *y*- and *z*-axes, respectively, with inner diameters of 0.5, 1.5, 2.5, and 3.5 μm. Figure 5(c) shows the potentials versus the *x*-axis with various inner diameters. At the end of the tip ($x = 0$) the potentials cannot be affected by van der Waals forces and a good trapping well can be obtained. Figure 5(d) shows the depth of the dipole trap versus the inner diameter. We also show the maximum depth for comparison (black solid squares). However, the effective depths in the *xy* (red solid circles) and *xz* planes (blue solid triangles) are much smaller than the maximum depth because of the effects of the tip body when the inner diameters are small. The effects of the tip body are reduced when the inner diameter increases. We eventually obtain the optimal peak trap depth of 0.82 mK when the ratio between the inner diameter and the outer diameter is 1.5:4 with an outer diameter of 4.0 μm.

We also optimize the outer diameters when the ratio between the inner and outer diameter is a constant, 1.5:4. The results are shown in figure 6. Figure 6(a) shows the FWHMs along the *y*- (black open squares) and *z*-axes (red open circles) as a function of inner diameter, 1.0, 2.0, 3.0, 4.0, and 5.0 μm. The FWHMs increase with increasing outer diameter. The working distance increases with increasing inner diameter (blue solid circles). We can see that a microcapillary tube tip with a larger outer diameter can give a longer working distance. Figure 6(b) shows the dipole trap depth versus the outer diameter. As a comparison, the maximum depth is also shown (black solid squares). The effective depths in the *xy* (red solid circles) and *xz* planes (blue solid triangles) are much smaller than the maximum depth because of the tip body effects when the inner diameter is small. Finally, we achieve the maximum trap depth of 1.14 mK when the outer diameter is 2.0 μm and the ratio between the inner diameter and the outer diameter is 1.5:4. From figure 6(a), the FWHMs in *xy* and *xz* planes are 0.85 μm and 0.67 μm, respectively, with the maximum trap depth of 1.14 mK. The subwavelength trap with this size 0.67 μm goes beyond the reported smallest trap yet today by using the conventional high numerical aperture optics [41], 0.84 μm.

The above results show that the microcapillary tube tip could be a good device for single atom trapping. The guided trapping light can propagate from a single mode fiber to the

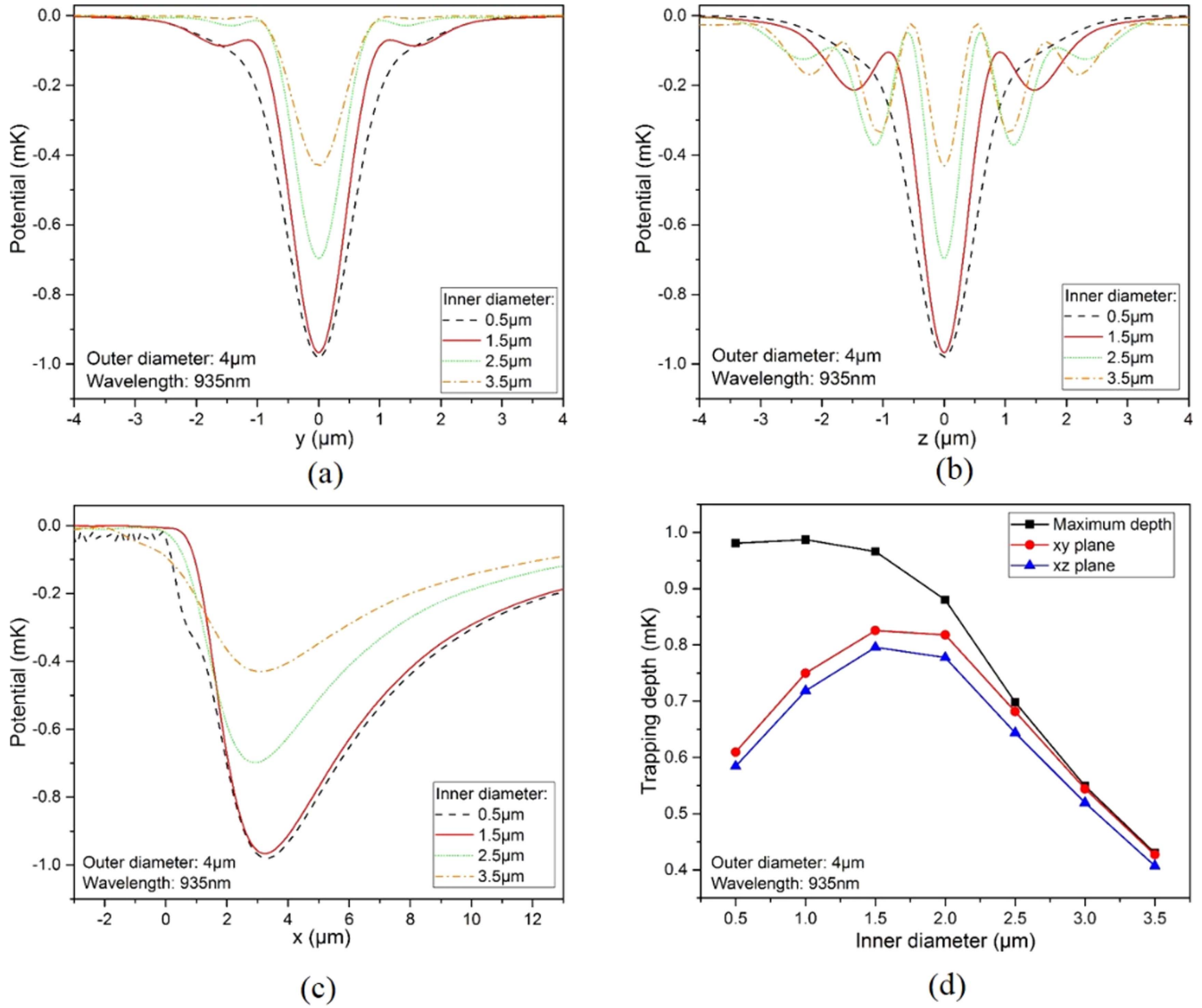

Figure 5. Simulation results for optimizing the inner diameter when the outer diameter is 4.0 μm. Trapping well potentials versus (a) *y*-axis and (b) *z*-axis with inner diameters of 0.5, 1.5, 2.5, and 3.5 μm. (c) Potentials versus *x*-axis with various inner diameters. (d) Depth of dipole trap as a function of the inner diameter. The maximum depth (black solid squares) and the effective depths in the *xy* (red solid circles) and *xz* planes (blue solid triangles) are shown in the panel for comparison.

tapered capillary tube tip by splicing the single mode fiber and the capillary tube. After splicing, the tapered micro-capillary can be fabricated using a commercial capillary pulling system or a microheater [41]. Alternatively, the tip can be fabricated by stretching a commercial capillary tube with the outer diameter few tens of micrometers by the flame-brush method, which is a usual method of fabricating micro/nanofibers [42]. The flat end of the tip can be cut by using a fiber cleaver or focused ion beam milling. Microcapillary tube tip imperfections caused by fabrication are inevitable. They may reduce the trapping depth of dipole traps formed by the microcapillary tube tip. To study the feasibility of this proposal we analyze the trapping depth reduced by two possible imperfections: roughness of cutting surface and cutting angle. We build a model which is a microcapillary tube tip with a rough cutting surface or an angled cutting. For the roughness of cutting surface, average rms amplitude (ARA) and average correlation length (ACL) of surface roughness are two key parameters to describe the roughness of a surface. Figure 7(a) shows simulations of the trapping depths as a function of the ARA when ACL is 0.1 μm. Figure 7(b) shows simulations of the trapping depths as a function of the ACL when ARA is 0.1 μm. The black solid squares are maximum depth and the red solid circles and blue solid triangles are effective depth in *xy* and *xz* planes. The effective depth in the *xy* plane decreases as the ARA or ACL are increased, while the effective depth in the *xz* plane increase a little bit when the ARA or ACL increases. The trapping depth as a function of the ARA and ACL show the same trend. In figure 7(a) the effective depth in *xy* plane is seen to decay to 1 mK when the ARA increases to 0.15 μm. It is easy to fabricate good surfaces with ARA and ACL smaller than 0.15 μm using focused ion beam milling with sub-nanometer precision. In brief, we can get a dipole trap with enough trapping depth (1 mK) for single atom

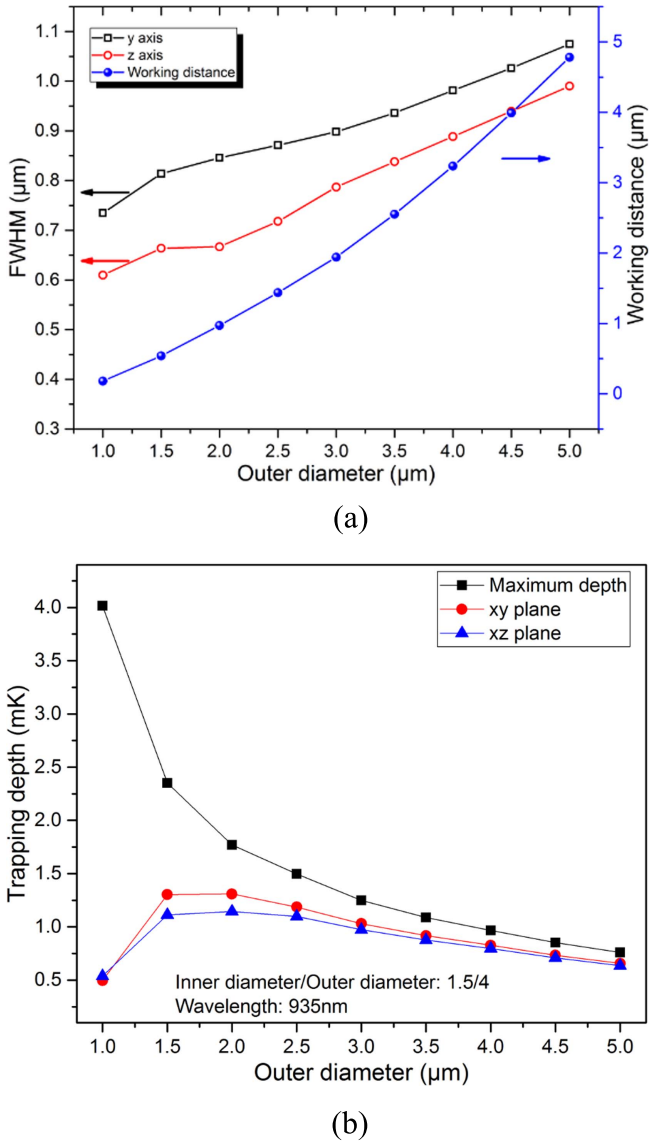

Figure 6. Simulation results for optimizing the outer diameter when the ratio between the inner and outer diameters is a constant, 1.5:4. (a) FWHM of the trapping well along the *y*-axis (black open squares) and *z*-axis (red open circles), and the working distance (blue solid circles) as a function of the outer diameter (1.0, 2.0, 3.0, 4.0, and 5.0 μm). (b) Depth of the dipole trap as a function of outer diameter. The maximum depth (black solid squares) and the effective depth in *xy* (red solid circles) and *xz* planes (blue solid triangles) are shown in the panel for comparison.

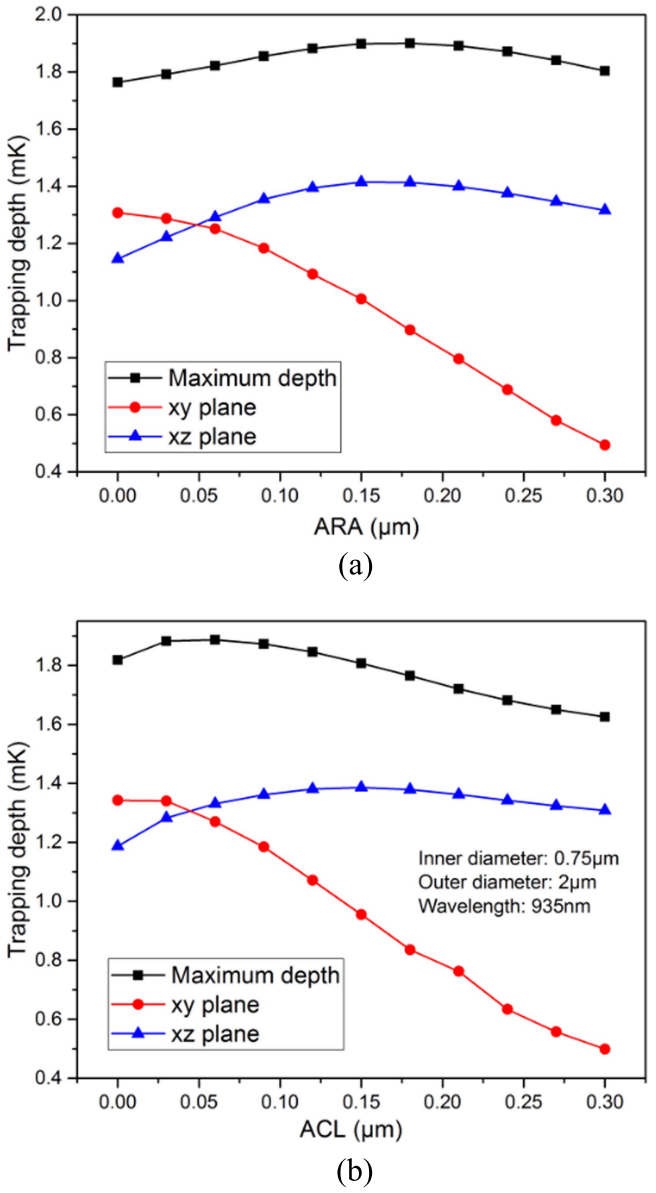

Figure 7. (a) Simulations of the trapping depths as a function of the ARA when ACL is 0.1 μm. (b) Simulations of the trapping depths as a function of the ACL when ARA is 0.1 μm. The maximum depth (black solid squares) and the effective depth in *xy* (red solid circles) and *xz* planes (blue solid triangles) are shown in the panel for comparison.

trapping using a microcapillary tube tip with an imperfect surface. In addition, higher optical dipole laser power can compensate trapping depth reduction due to an imperfect surface of microcapillary tube tip. Except for roughness of surface, it is not easy to keep the end surface of microcapillary tube tip perpendicular to the axis of tube during the fabrication, especially when the diameter of tube is just few microns. To estimate the effect of this imperfection we vary the angle between tube axis and normal line of end surface, called cutting angle, from 0 to 45 degree. The result is shown in figure 8. We can see that effective depths in *xy* and *xz* planes keep constant when the cutting angle is less than 16 degrees, while they decay rapidly when the angle is more than 25 degrees. We can get the trapping depth to be more than 1 mK when the cutting angle is smaller than 25 degrees. The controllable fabrication imperfections shown above would not affect the performance of the scheme.

The microcapillary tube tip can collect the fluorescence of single atoms trapped efficiently and thus single trapped atoms can be detected by using fluorescence collections. We have simulated the collection efficiency of a single atom using the FDTD method and the collection efficiency can reach 19% which is much higher than reported in [12]. In addition, the position of the trapped single atoms can be controlled precisely by moving the microcapillary tube tips. The

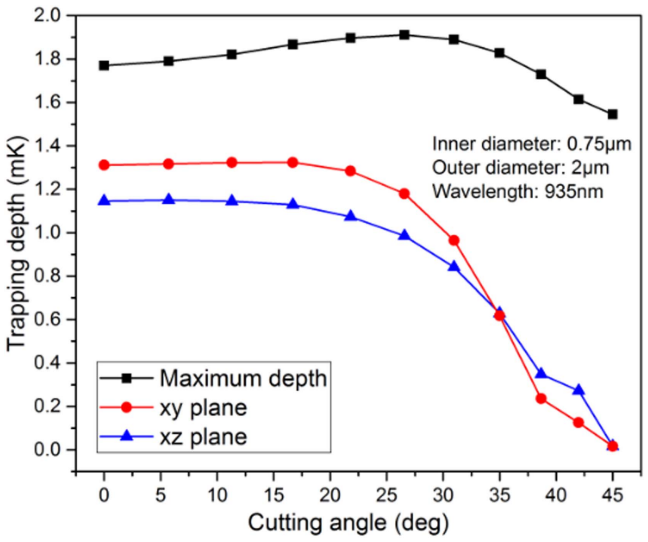

Figure 8. Simulations of the trapping depths as a function of the cutting angle. The maximum depth (black solid squares) and the effective depth in *xy* (red solid circles) and *xz* planes (blue solid triangles) are shown in the panel for comparison.

fabrication of a microcapillary tube tip for single atom trapping is underway.

In conclusion, we have given a feasible scheme of a state-insensitive dipole trap for single neutral cesium atoms by a microcapillary tube tip. The results show that a microcapillary tube tip with an outer diameter of about 2.0 μm and ratio between the inner diameter and the outer diameter 1.5:4 can confine a trapping light tightly and form a trapping well with depth of 1.14 mK. The full width at half-maximum of the trapping well can reach 0.67 μm. The subwavelength-trap can be used to control single atoms with more confinement, while large distances between the trap and tip surface avoids the effects of van der Waals forces. Microcapillary tube tips of a few micrometers in diameter can provide a 1 mK dipole trap with an optical power of only 6 mW. The effects of two imperfections, roughness of end surface and cutting angle of microcapillary tube tip, are estimated. We can get enough trapping depth for single atom trapping, 1 mK, when the ARA and ACL is less than 0.15 μm and the cutting angle is less than 16 degrees. The tips with the order of micrometer size are small enough to be combined with micro/nano structures. Hybrid systems combining single atom trapping and micro/nano structures have become useful and significant candidates for integration technology and quantum networks, which are important elements of quantum information processing.

Acknowledgments

The work is supported by the National Nature Science Foundation of China (Project No. 11574187, 11204165, 11634008, 11674203, 61227902) and the Major State Basic Research Development Program of China.

References

[1] Grangier P, Sanders B and Vuckovic J 2004 Focus on single photons on demand *New J. Phys.* **6** 1367–2630
[2] Volz J, Weber M, Schlenk D, Rosenfeld W, Vrana J, Saucke K, Kurtsiefer C and Weinfurter H 2006 Observation of entanglement of a single photon with a trapped atom *Phys. Rev. Lett.* **96** 030404
[3] Jones M P A, Beugnon J, Gaëtan A, Zhang J, Messin G, Browaeys A and Grangier P 2007 Fast quantμm state control of a single trapped neutral atom *Phys. Rev.* A **75** 040301(R)
[4] Nielsen M A and Chuang I L 2000 *Quantum Computation and Quantum Information* (Cambridge: Cambridge University Press)
[5] Monroe C and Lukin M 2008 Remapping the quantum frontier *Phys. World* **21** 32–9
[6] Wallquist M, Hammerer K, Rabl P, Lukin M and Zoller P 2009 Hybrid quantum devices and quantum engineering *Phys. Scr.* **T137** 014001
[7] Murphy B and Hau L V 2009 Electro-optical nanotraps for neutral atoms *Phys. Rev. Lett.* **102** 033003
[8] Thompson J D, Tiecke T G, Leon N P, Feist J, Akimov A V, Gullans M, Zibrov A S, Vuletić V and Lukin M D 2013 Coupling a single trapped atom to a nanoscale optical cavity *Science* **340** 1202–5
[9] Hung C L, Meenehan S M, Chang D E, Painter O and Kimble H J 2013 Trapped atoms in one-dimensional photonic crystals *New J. Phys.* **15** 083026
[10] Kato S and Aoki T 2015 Strong coupling between a trapped single atom and an all-fiber cavity *Phys. Rev. Lett.* **115** 093603
[11] Grimm R, Weidemuller M and Ovchinnikov Y B 2000 Optical dipole traps for neutral atoms *Adv. At. Mol. Opt. Phys.* **42** 95–170
[12] Guo Y, Li G, Zhang Y, Zhang P, Wang J and Zhang T 2012 Efficient fluorescence detection of a single neutral atom with low background in a microscopic optical dipole trap *Science in China* **55** 1523–8
[13] Schlosser N, Reymond G, Protsenko I and Grangier P 2001 Sub-poissonian loading of single atoms in a microscopic dipole trap *Nature* **411** 1024–7
Sortais Y R P *et al* 2007 Diffraction-limited optics for single-atom manipulation *Phys. Rev.* A **75** 013406
[14] Wang J L, Li G, Tian Y L and Zhang T C 2015 Measurement and 3D reconstruction of the micro-scale optical dipole trap for single atom manipulation *J. Quantum Opt.* **21** 74
[15] Ovchinnikov Y B, Shulga S V and Balykin V I 1991 An atomic trap based on evanescent light waves *J. Phys.* B **24** 3173–8
[16] Hammes M, Rychtarik D, Engeser B, Nagerl H C and Grimm R 2003 Evanescent-wave trapping and evaporative cooling of an atomic gas at the crossover to two dimensions *Phys. Rev. Lett.* **90** 173001
[17] Kien F L, Balykin V I and Hakuta K 2004 Atom trap and waveguide using a two-color evanescent light field around a subwavelength-diameter optical fiber *Phys. Rev.* A **70** 063403
[18] Vetsch E, Reitz D, Sagué G, Schmidt R, Dawkins S T and Rauschenbeutel A 2010 Optical interface created by laser-cooled atoms trapped in the evanescent field surrounding an optical nanofiber *Phys. Rev. Lett.* **104** 203603
[19] Goban A, Choi K S, Alton D J, Ding D, Lacroûte C, Pototschnig M, Thiele T, Stern N P and Kimble H J 2013 Demonstration of a state-insensitive compensated nanofiber trap *Phys. Rev. Lett.* **109** 033603
[20] Daly M, Truong V G, Phelan C F, Deasy K and Chormaic S N 2014 Nanostructured optical nanofibres for atom trapping *New J. Phys.* **16** 053052

[21] Kien F L and Hakuta K 2009 Microtraps for atoms outside a fiber illuminated perpendicular to its axis numerical results *Phys. Rev.* A **80** 013415
[22] Goban A, Hung C L, Hood J D, Yu S P, Muniz J A, Painter O and Kimble H J 2015 Superradiance for atoms trapped along a photonic crystal waveguide *Phys. Rev. Lett.* **115** 063601
[23] Garcia S, Maxein D, Hohmann L, Reichel J and Long R 2013 Fiber-pigtailed optical tweezer for single-atom trapping and single-photon generation *Appl. Phys. Lett.* **103** 114103
[24] Ashkin A 1970 Acceleration and trapping of particles by radiation pressure *Phys. Rev. Lett.* **24** 156–9
[25] Lyons E R and Sonek G J 1995 Confinement and bistability in a tapered hemispherically lensed optical fiber trap *Appl. Phys. Lett.* **66** 1584–6
[26] Numata T, Takayanagi A, Otani Y and Umeda N 2006 Manipulation of metal nanoparticles using fiber-optic laser tweezers with a microspherical focusing lens *Jpn. J. Appl. Phys.* **45** 359–63
[27] Liu Z, Guo C, Yang J and Yuan L 2006 Tapered fiber optical tweezers for microscopic particle trapping: fabrication and application *Opt. Express* **14** 12510–6
[28] Valkai S, Oroszi L and Ormos P 2009 Optical tweezers with tips grown at the end of fibers by photopolymerization *Appl. Opt.* **48** 2880–3
[29] Black J B, Luo D and Mohanty S K 2012 Fiber-optic rotation of micro-scale structures enabled microfluidic actuation and self-scanning two-photon excitation *Appl. Phys. Lett.* **101** 221105
[30] Mondal S K, Pal S S and Kapur P 2012 Optical fiber nano-tip and 3D bottle beam as non-plasmonic optical tweezers *Opt. Express* **20** 16180–5
[31] Liu Z, Wang L, Liang P, Zhang Y, Yang J and Yuan L 2013 Mode division multiplexing technology for singlefiber optical trapping axial-position adjustment *Opt. Lett.* **38** 2617–20
[32] Barron A L, Kar A K, Aspray T J, Waddie A J, Aghizadeh M R and Bookey H T 2013 Two dimensional interferometric optical trapping of multiple particles and escherichia coli bacterial cells using a lensed multicore fiber *Opt. Express* **21** 13199–207
[33] Decombe J B, Huant S and Fick J 2013 Single and dual fiber nano-tip optical tweezers: trapping and analysis *Opt. Express* **21** 30521–31
[34] Chang D E, Thompson J D, Park H, Vuletic´ V, Zibrov A S, Zoller P and Lukin M D 2009 Trapping and manipulation of isolated atoms using nanoscale plasmonic structures *Phys. Rev. Lett.* **103** 123004
[35] Fu J, Dong H and Fang W 2010 Subwavelength focusing of light by a tapered microtube *Appl. Phys. Lett.* **97** 041114
[36] Kato S, Chonan S and Aoki T 2014 High-numerical-aperture microlensed tip on an air-clad optical fiber *Opt. Lett.* **39** 773–6
[37] Derevianko A 2010 Theory of magic optical traps for zeeman-insensitive clock transitions in alkali-metal atoms *Phys. Rev.* A **81** 051606(R)
[38] Degenhardt C, Stoehr H, Sterr U and Riehle F 2004 Wavelength-dependent ac stark shift of the $^1S_0$-$^3P_1$ transition at 657 nm in Ca *Phys. Rev.* A **70** 023414
[39] Steck D A 2003 Cesium D Line Data; Kurucz R L and Bell B 1995 Atomic Line Data. Kurucz CD-ROM No. 23
[40] McLachlan A D 1964 Van der Waals forces between an atom and a surface *Mol. Phys.* **7** 381–8
[41] Kaufman A M, Lester B J, Reynolds C M, Wall M L, Foss-Feig M, Hazzard K R A, Rey A M and Regal C A 2014 Two-particle quantum interference in tunnel-coupled optical tweezers *Science* **345** 306–9
[42] Birks T A and Li Y W 1992 The shape of fiber tapers *J. Lightwave Tech.* **10** 432–8